Sub-parts-per-billion level detection of NO_2 using room-temperature quantum cascade lasers

Michael Pushkarsky*, Alexei Tsekoun*, Ilya G. Dunayevskiy*, Rowel Go*, and C. Kumar N. Patel*†‡

*Pranalytica, Inc., 1101 Colorado Avenue, Santa Monica, CA 90401; and †Department of Physics and Astronomy, University of California, Los Angles, CA 90095

Contributed by C. Kumar N. Patel, May 24, 2006

We report the sub-parts-per-billion-level detection of NO_2 using tunable laser-based photoacoustic spectroscopy where the laser radiation is obtained from a room-temperature continuous-wave high-power quantum cascade laser operating in an external grating cavity configuration. The continuously tunable external grating cavity quantum cascade laser produces maximum single-frequency output of ≈300 mW tunable over ≈350 nm centered at 6.25 μm. We demonstrate minimum detection level of ≈0.5 parts per billion of NO_2 in the presence of humidified air.

IR lasers | NO_2 spectroscopy | photoacoustic spectroscopy | sub-parts-per-billion detection of gases

Real-time trace-level gas detection is an area of fast growth with applications in such diverse fields as medical diagnostics, process control, national security, and environmental air-quality monitoring. Techniques based on the measurement of optical absorption using tunable laser sources are attractive detection methods because of their intrinsic sensitivity and selectivity, i.e., an ability for discriminating against interferents (1, 2). The most recent advances, intercomparison of spectroscopic techniques, and status of available laser sources are summarized in a recent review (3). Furthermore, photoacoustic (PA) spectroscopy is seen to be well suited for optical absorption measurements because it combines high sensitivity with the ruggedness needed for field-deployable instrumentation. However, laser PA spectroscopy (L-PAS) requires multihundred-milliwatt-level laser sources to achieve a sub-parts-per-billion (sub-ppb) level of sensitivity for many of the environmentally and industrially important gases. As a result, heretofore most of the sensitive L-PAS detection schemes have used continuous-wave (CW) molecular gas lasers (4).

Results and Discussion

High-Power Continuously Tunable Laser Source. The tuning characteristics of our high-power single-frequency source are seen in Fig. 1, which shows the single-mode laser power available from the CW room temperature (RT) external grating cavity (EGC) quantum cascade laser (QCL) (near 6.3 μm) at several grating settings. Fig. 1 also shows the overall tuning of the output that covers >350 nm with CW RT laser power in excess of ≈200 mW with maximum CW RT laser power of 300 mW near the center of the tuning curve. Details are given in *Materials and Methods*.

PA Spectroscopy of NO_2. We have used the broadly and continuously tunable, high-power CW RT EGC-QCL source for PA spectroscopy of NO_2, which exhibits strong absorption features near ≈1,600 cm^{-1}. NO_2 is a smog and particulate matter precursor and one of the key pollutants that is routinely monitored. Ambient concentrations of NO_2 typically are in single digits to tens of parts per billion (ppb) levels (5). The national ambient air quality standard (NAAQS) level for NO_2 is 53 ppb for arithmetic mean average (6). Consequently, an acceptable ambient NO_2 sensor should have single-digit ppb or, better, sub-ppb, sensitivity. Earlier, cryogenically cooled lead salt lasers (7) operating near 6.3 μm had been used to demonstrate low-hundred parts-per-trillion sensitivity detection of NO_2 using direct multipass absorption spectroscopy.

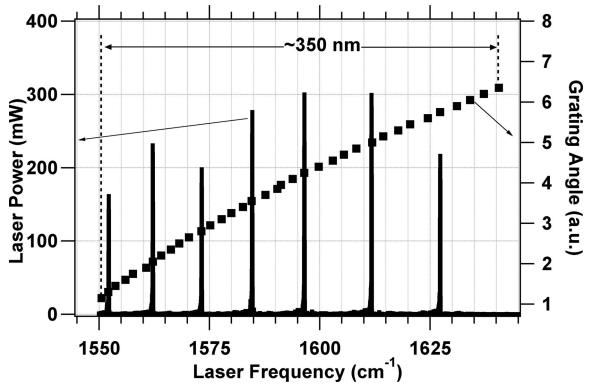

Fig. 1. Fourier transform IR spectra of EGC-QCL single-mode laser output recorded at several diffraction grating angles and the tuning behavior as a function of the grating angle. The highest measured single-mode power is ≈300 mW.

To obtain PA spectra of NO_2, the collimated EGC-QCL output was directed into a PA cell as described in ref. 4. Laser amplitude modulation was achieved by using a mechanical chopper, and the modulation frequency was adjusted to coincide with the first longitudinal resonance of the PA cell at ≈1,800 Hz. Upon leaving the cell, a fraction of the laser beam was measured using an uncooled HgCdTe detector for normalization purposes. The PA cell microphone output signal and the IR detector signal were analyzed by using a pair of lock-in amplifiers, keeping track of in-phase and out-of-phase components of the signals.

Ambient NO_2 sensing at 6.3 μm is often complicated by potential interference from water vapor. To demonstrate sensor performance in realistic conditions, the spectra were recorded both in clean dry air (CDA) and in air with added 0.85% absolute humidity (corresponding to ≈28% relative humidity at 25°C). Controlled concentrations of NO_2 were produced by mixing the output of the NO_2 permeation device with a balance of either CDA or CDA bubbled through an impinger filled with water maintained at 5°C. Keeping the PA cell pressure at (or below) 250 torr (1 torr = 133 Pa) permits L-PAS to minimize the water vapor interference. The gas sample was continuously introduced in the PA cell at a flow rate of ≈75 standard cubic cm/min (sccm).

L-PAS spectra of water vapor and NO_2 in humidified air, recorded in the spectral range of ≈1,600 cm^{-1}, are shown in Fig.

Conflict of interest statement: No conflicts declared.

Freely available online through the PNAS open access option.

Abbreviations: CW, continuous wave; EGC, external grating cavity; PA, photoacoustic; L-PAS, laser PA spectroscopy; QCL, quantum cascade laser; RT, room temperature; CDA, clean dry air; FP, Fabry–Perot; ppb, parts per billion.

‡To whom correspondence should be addressed. E-mail: patel@pranalytica.com.

www.pnas.org/cgi/doi/10.1073/pnas.0604238103

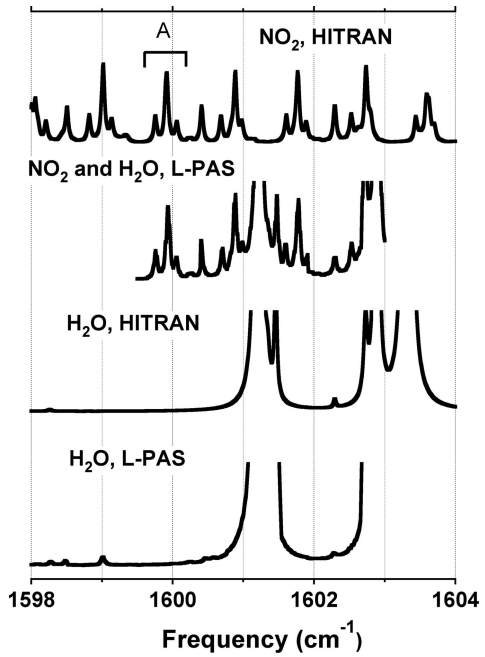

Fig. 2. Simulated HITRAN database and experimental L-PAS spectra of water vapor and nitrogen dioxide at 250 torr. A strong NO_2 triplet at 1,599.9 cm^{-1} (labeled A) is free from water interference.

2 along with the HITRAN (for high-resolution transmission) molecular absorption database (ref. 8; www.HITRAN.com) simulations. The region contains several strong NO_2 spectral features, which according to both the HITRAN database and experiment are free of water interference. A triplet spectral feature of NO_2 (labeled A in Fig. 2), centered at 1,599.95 cm^{-1} and seen to be water-interference free, was used to evaluate the sensitivity of our technique for detecting NO_2.

Sub-ppb Detection of NO_2. Short scans around the selected spectral region were obtained for several NO_2 concentrations in CDA ranging from 10.4 ppm to 100 ppb, the lowest value being limited by the dynamic range of the our gas-mixing system. The L-PAS signal at each point was recorded with a lock-in amplifier time constant of 10 ms and integration time of 1 s. Fig. 3 shows spectral traces for NO_2 concentrations of 10.4 ppm and 100 ppb. The 10.4-ppm trace was taken with intentionally small step size (0.002 cm^{-1}) to illustrate the resolution of the EGC-QCL

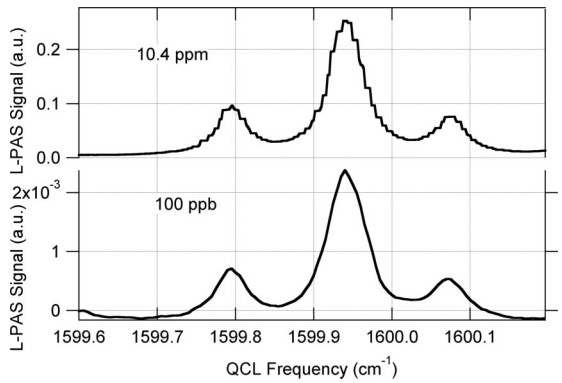

Fig. 3. L-PAS scans across the selected NO_2 spectral feature (A in Fig. 2) in CDA. The upper trace shows 10.4 ppm NO_2. The step changes in the signal intensity are due to external cavity mode hops. The lower trace shows five point-averaged 100-ppb NO_2 data (see text).

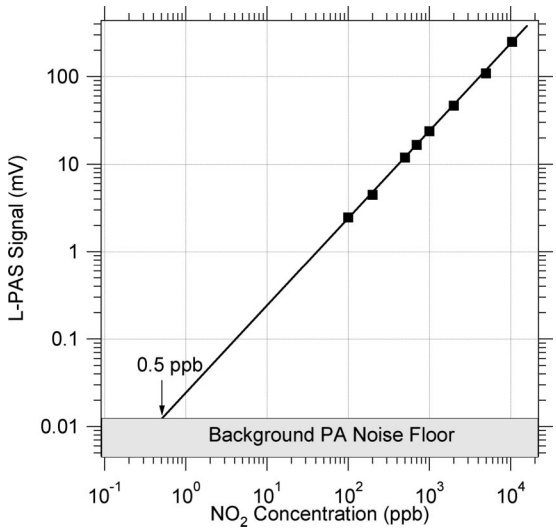

Fig. 4. NO_2 L-PAS linearity. Unity signal-to-noise ratio corresponds to the 0.5-ppb NO_2 detection limit (grayed-out area).

tunability. The effects of external cavity mode hops are seen as small steps in the line profile of the laser power normalized L-PAS spectrum. The 100-ppb trace was recorded with coarser frequency step size (0.005 cm^{-1}) to keep total spectral acquisition time reasonably short (120 s) and digitally averaged over five points for presentation purposes. Fig. 4 shows L-PAS response linearity for several NO_2 concentrations from 10.4 ppm to 100 ppb. The 100-ppb trace reveals a nearly constant background attributed primarily to the cell heating resulting from the laser light reflected and absorbed by the L-PAS cell windows. The noise level and associated sensor sensitivity were estimated by an analysis of the noise at the beginning and end of the recorded 100-ppb trace of NO_2 and separately by an analysis of the spectra of CDA with no NO_2 present. Background noise level is equivalent to 0.5 ppb of NO_2 (1σ) and arises predominantly from the electrical noise of the cell microphone. This sensitivity value comfortably fits with the requirements for an ambient NO_2 sensor.

Although water vapor absorption does not interfere with NO_2 sensing at transitions selected for this study, water vapor concentration affects both amplitude and phase of the NO_2 L-PAS signal as shown in Fig. 5. The amplitude of the L-PAS signal increases with the water content and levels off at >0.5% absolute humidity level, with signal approximately three times that in dry air. The phase of NO_2 signal also changes from dry air to 1% absolute humidity, a clear indication of relaxation effects (9). Therefore, a QCL-PAS-based ambient NO_2 sensor will require a simultaneous humidity measurement, most conveniently ac-

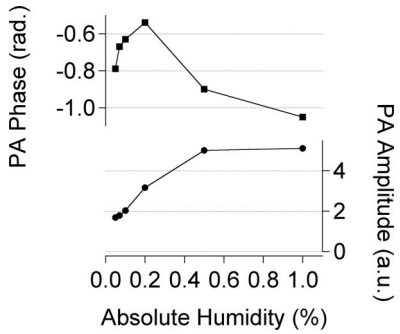

Fig. 5. Dependence of NO_2 L-PAS amplitude and phase on humidity content.

complished by measuring a nearby strong water absorption line in the same spectral trace (Fig. 2) and normalizing the NO_2 signal by a proper factor, depending on the humidity level.

Conclusions

In conclusion, this letter reports a demonstration of a previously undescribed broadly and continuously tunable, high-power CW EGC-QCL laser source operating at RT and its suitability for ambient level nitrogen dioxide detection in air. The demonstration of a previously undescribed high-power CW RT semiconductor laser source in mid-IR suitable for gas sensing bridges the most urgent technology gap in the development of a new generation of field-deployable optical absorption-based sensors.

Materials and Methods

High-Power CW Operating RT QCLs. Recent advances in the fabrication and packaging of QCLs have yielded devices capable of emitting as much as 0.5 W of CW power at RT in Fabry–Perot (FP) geometry in the 4.5- to 8-μm region (10, 11). In the present work, we report the development of a mode-hop free, broadly and continuously tunable CW RT high-power EGC-QCL source operating in the 6.3-μm region and demonstrate high-sensitivity L-PAS detection of NO_2 by using this source.

QCL ridge waveguide gain chips, fabricated by the Center for Quantum Devices at Northwestern University (Evanston, IL) with gain region centered at $\approx$6.3 μm, were mounted by using epi-side-down bonding on AlN submounts with AuSn eutectic solder (11). Chip cavity length was 4 mm, and crystal facets were not coated. The chip on the submount was integrated onto a copper heat spreading pyramid with a thermoelectric cooler (TEC) and a miniature copper cooling block for heat removal from the hot side of the TEC. The cooling block is presently water-cooled but may be modified for forced-air cooling. The gain chips were operated at an actively controlled submount temperature, $T_{\text{submount}} = 25$°C, measured by an integrated thermistor, with the copper cooling block also maintained at 25°C.

Continuous Tuning of EGC-QCLs. To achieve single-mode operation and wavelength tunability, an EGC setup composed of discrete optical components was used. The output from the back facet of the gain chip was collimated by using either a f/1.0, 25-mm diameter off-axis parabolic mirror or a f/0.7 aspheric antireflection-coated ZnSe collimating lens [where f/n = (focal length of lens)/diameter of lens)]. In the case of ZnSe lens, beam diameter was $\approx$4 mm. The resulting collimated beam was reflected off a plane, high-efficiency, 300-lines-per-mm diffraction grating in Littrow configuration. To compensate for the decreased resolving power of the grating due to decreased beam diameter when the ZnSe lens was used, the grating in those experiments was configured in a double-pass geometry. The grating incidence angle could be precisely and reproducibly adjusted by using a computer-controlled linear actuator with an integrated encoder. The grating was attached to its rotational mount with a piezoelectric linear translator to enable fine adjustments of the external cavity length.

Because the back facet of the gain chip was uncoated, we encountered the usual coupled cavity problem (12), where the spectral output is governed by the FP modes of the gain chip as well as the modes of the overall external cavity. To minimize the effect of spectral mode hops across the modes of the external cavity, we selected a long external cavity of $\approx$1 m, yielding FP mode spacing of $\approx$150 MHz. With such an external cavity, the spectral output, although not continuously tunable in the strictest sense, exhibits at most $\pm$75 MHz variations from the precise resonant frequency of a given FP mode of the laser chip. Compared with the characteristic width of spectroscopic features studied in this work, this step size is very small, and for the purposes of the present studies the laser source may be treated as continuously tunable. With an aspheric lens as a collimator, we were able to achieve single-mode operation over a tunability range of 350 nm, limited by weakening of the gain and the reversion of laser output to FP modes of the gain chip even in the presence of feedback. The single-mode CW output power in the center of the gain curve at maximum current was 300 mW. Fig. 1 shows single-mode spectral output of the 6.3-μm external cavity QCL at several grating angles together with the overall tuning of the output frequency.

To achieve continuous wavelength scanning over a broad spectral range in the presence of coupled cavity effects, substantial modification and expansion of the existing simultaneous current/grating tuning algorithm (13) were necessary. In this scheme, the FP wavelength comb of the gain chip was shifted spectrally by varying the laser chip injection current, and the grating angle was simultaneously adjusted to keep a selected single-chip FP mode at the minimum of the diffraction grating-induced loss, thus ensuring selective lasing at that mode only.

However, this approach presents a serious limitation on the overall tuning range, namely the limited dynamic range of the laser injection current. For typical QCL gain chips that we studied, the total current span between laser threshold and the maximum rated laser current were sufficient to shift the FP comb by somewhat less than 3 cm^{-1}, thus putting an upper limit on the mode hop-free tuning range. In a practical spectroscopic instrument, where one needs to maintain a reasonably high laser power level to achieve the desired sensitivity, the actual tuning range could become <1 cm^{-1}.

To circumvent this problem, we have developed a previously undescribed method for periodically varying the laser injection current to achieve a continuous shift of the gain chip's FP comb, thus enabling mode hop-free tuning over a wide spectral range. In our method, we first determined the current value necessary to shift the FP comb exactly one free spectral range (FSR) of the gain chip. We made this determination by analyzing high-resolution Fourier transform infrared (FTIR) spectra of the gain chip in the absence of external cavity; however, other mechanisms are also possible. Then, as the laser is tuned in the external cavity geometry, the software algorithm calculates nominal laser current value necessary to have one of the gain chip's FP modes exactly coincide with the desired output frequency. Depending on the constants of the simultaneous current-grating tuning algorithm (described below), this value may be entirely unphysical, i.e., above maximum permissible laser current or negative. However, given the periodic nature of current tuning, our software algorithm remaps this nominal laser drive current value onto a value in the optimum current window, typically selected to have maximum permissible laser current as its upper boundary. Then, as the laser is tuned so that the nominal current value is about to become more than one periodicity value below maximum laser current, the current is recalculated and set back to a value close to maximum. This process continues periodically as the laser is broadly tuned, completely removing the tuning range restriction that the limited dynamic range of the current would otherwise impose. It is clear that the manipulation of laser temperature to shift gain chip FP modes presents the same dynamic range problem. However, it can be accommodated in a periodic fashion similar to that described for current here. Furthermore, even though we built our broadly tunable laser using QCL gain chips, our technique is directly translatable to an external cavity (EC) system using any type of semiconductor laser as its gain medium.

Numerical values of tuning constants were obtained through characterizing the output of the EGC-QCL with a high-resolution FTIR spectrometer. The output spectra were recorded under two conditions: (*i*) various driving current values and a fixed grating angle, and (*ii*) several grating angles with fixed current. The gain chip was maintained at a constant temperature

of 25°C. In both cases, the laser output exhibited regions of single-mode operation, interleaved with the regions of mode hops between adjacent FP modes. Simultaneous current-grating tuning was able to bridge the spectral gaps between FP modes of the gain chip and resulted in continuous single-mode frequency coverage. In the final arrangement, the EGC setup was operated under computer control, where the algorithm selected and set the required laser injection current and grating angle for the desired QCL output frequency. We obtained an overall tuning range of ≈350 nm centered at ≈1,600 cm^{-1} (Fig. 1), with maximum single-frequency optical power of 300 mW. Continuous tuning was demonstrated by recording actual gas spectra over ≈20 nm (Fig. 2) with absolute frequency error of no more than 1 GHz. Further, continuous tuning was confirmed by recording FTIR spectra in several additional randomly selected subregions of the overall tuning window, spanning multiple free spectral ranges of the QCL gain chip. This method allowed us to conclude that our external cavity laser source was continuously tunable in the entire 350-nm tuning window. Our results represent substantial improvement over those reported recently (14), where an EGC-QCL operating at a temperature below −20°C generated ≤1 mW of CW power at ≈5.2 μm and exhibited mode hop-free tuning over ≈1.2 cm^{-1} and coarse tuning over ≈90 nm.

This work was supported in part through Defense Advanced Research Planning Agency Contract HR0011-04-C-0102.

1. Webber, M., Pushkarsky, M. & Patel, C. K. N. (2005) *J. Appl. Phys.* **97,** 113101.
2. Webber, M., Pushkarsky, M., Macdonald, T. & Patel, C. K. N. (2006) *Appl. Phys. Lett.* **88,** 044103.
3. Tittel, F., Richter, D. & Fried, A. (2003) *Solid-State Mid-Infrared Laser Sources*, Topics in Applied Physics, eds. Sorokina, I. T. & Vodopyanov, K. L. (Springer, New York), Vol. 89, pp. 445–510.
4. Pushkarsky, M., Weber, M. & Patel, C. K. N. (2003) *Appl. Phys. B* **77,** 381–385.
5. Environmental Protection Agency (2003) *EPA National Air Quality and Emission Trends Report: 2003 Special Studies Edition* (Environ. Protection Agency, Research Triangle Park, NC), EPA Publ. No. 454/R-03-005.
6. 61 *Federal Register* 196 (1996).
7. Horii, C., Zahniser, M., Nelson, D., McManus, J. & Wofsy, S. (1999) *SPIE Proc.* **3758,** 152–161.
8. Rothman, L., Barbe, A., Benner, D., Brown, L., Camy-Peyret, C., Carleer, M., Chance, K., Clerbaux, C., Dana, V., Devi, V., *et al.* (2003) *J. Quant. Spectrosc. Radiat. Transfer* **82,** 5–44.
9. Moeckli, M., Hilbes, C. & Sigrist, M. (1998) *Appl. Phys. B* **67,** 449–458.
10. Evans, A., Yu, J., David, J., Doris, L., Mi, K., Slivken, S. & Razeghi, M. (2004) *Appl. Phys. Lett.* **84,** 314–316.
11. Tsekoun, A., Go, R., Pushkarsky, M., Razeghi, M. & Patel, C. K. N. (2006) *Proc. Natl. Acad. Sci. USA* **103,** 4831–4835.
12. Genty, G., Grohn, A., Talvitie, H., Kaivola, M. & Ludvigsen, H. (2000) *IEEE J. Quantum Electron.* **36,** 1193–1198.
13. Pilgrim, J. & Oh, D. (2004) U.S. Patent 6,683,895 B2.
14. Wysocki, G., Curl, R., Tittel, F., Maulini, R., Billiard, J. & Faist, J. (2005) *Appl. Phys. B* **81,** 769–777.